Letter

Improving force sensitivity by amplitude measurements of light reflected from a detuned optomechanical cavity

Kentaro Komori,[1,2,*] Takuya Kawasaki,[1] Sotatsu Otabe,[3] Yutaro Enomoto,[4] Yuta Michimura,[1] and Masaki Ando[1]

[1]*Department of Physics, University of Tokyo, Bunkyo, Tokyo 113-0033, Japan*

[2]*Institute of Space and Astronautical Science, Japan Aerospace Exploration Agency, Sagamihara, Kanagawa 252-5210, Japan*

[3]*Department of Physics, Tokyo Institute of Technology, Meguro, Tokyo 152-8550, Japan*

[4]*Department of Applied Physics, School of Engineering, The University of Tokyo, 7-3-1 Hongo, Bunkyo-ku, Tokyo 113-8656, Japan*

(Received 25 May 2021; accepted 19 August 2021; published 2 September 2021)

The measurement of weak continuous forces exerted on a mechanical oscillator is a fundamental problem in various physical experiments. It is fundamentally impeded by quantum back-action from the meter used to sense the displacement of the oscillator. In the context of interferometric displacement measurements, we here propose and demonstrate the working principle of a scheme for coherent back-action cancellation. By measuring the amplitude quadrature of the light reflected from a detuned optomechanical cavity inside which a stiff optical spring is generated, back-action can be canceled in a narrow band of frequencies. This method provides a simple way to improve the sensitivity in experiments limited by quantum back-action without injection of squeezed light or stable homodyne readout.

DOI: 10.1103/PhysRevA.104.L031501

I. INTRODUCTION

Precise mechanical sensing of forces has a long history, and a rich future. In the past, that pursuit has been exemplified by tests of Newtonian gravity [1–5], nanomechanics-based force microscopy [6,7], and gravitational-wave detection using kilogram-scale test masses [8,9]. The integration of nanoscale mechanical oscillators with optical cavities—within the field of cavity optomechanics [10,11]—has opened the possibility of addressing a new set of questions through precision mechanical sensing. Examples include tests of gravitational effects in quantum mechanics [12–16], tests of fundamental decoherence phenomena [17–22], and dark matter detection [23–27]. The common denominator in all these quests is the precise measurement of forces acting on mechanical oscillators.

The estimation of weak continuous forces is fundamentally limited by quantum noise. When optical fields are used to measure the displacement of a mechanical force transducer, vacuum fluctuations in the former produce a fluctuating back-action force that can obscure an external force [28]. Such quantum back-action can be reduced by injection of light whose quadratures are squeezed in a frequency-dependent fashion [29–34], or by employing ponderomotively generated squeezed light [35–38]. In the context of force detection, the standard quantum limit (SQL) in the free-mass regime [39] $S_F^{\mathrm{SQL}}(\omega) = 2\hbar m\omega^2$ decreases with decreasing frequency. Yet the opportunity for high precision force sensing is thwarted by the inability to generate squeezed light at low frequencies and/or phase noise in homodyne detection (as required for schemes that rely on ponderomotive squeezed light).

In this Letter, we theoretically describe and experimentally demonstrate the principle of a technique that can circumvent both these technical problems. In particular, we show that direct amplitude detection of the light reflected from a detuned optomechanical system can realize quantum noise cancellation around the optical spring frequency. Working in reflection has the fundamental advantage of the better sensitivity with an overcoupled cavity and beating the SQL, in contrast to similar schemes that operate in transmission [40]. Our scheme also does not require squeezed light or phase-stable homodyne detection to produce force sensitivities beyond the SQL. We also demonstrate the principle behind this scheme by showing that classical intensity noise in the laser used to probe the optomechanical system is suppressed in a manner consistent with theory.

II. PRINCIPLE OF QUANTUM NOISE CANCELLATION IN AMPLITUDE READOUT

We consider a Fabry-Perot cavity with a mechanically compliant end mirror of transmissivity t_{out} and reflectivity $r_{\mathrm{out}} = \sqrt{1 - t_{\mathrm{out}}^2}$, and a fixed input mirror of transmissivity t_{in} and reflectivity $r_{\mathrm{in}} = \sqrt{1 - t_{\mathrm{in}}^2}$. All optical loss in the system is modeled as being due to the nonzero transmissivity of the end mirror. Adopting the two-photon formalism [41,42], we consider each optical field in the inset in Fig. 1 as being composed of a pair of quadratures; e.g., $\boldsymbol{a} = (a_1\ a_2)^t$, where a_1 (a_2) is an amplitude (phase) quadrature of the intracavity light. Other fields are defined as shown in the inset: $\boldsymbol{b}$ ($\boldsymbol{c}$) is going into (out from) the input mirror, and $\boldsymbol{d}$ ($\boldsymbol{e}$) is going into (out from) the end mirror. The displacement caused by the external force can be read out by $\boldsymbol{c}$ or $\boldsymbol{e}$ with the carrier. The cavity amplification matrix between the amplitude and phase of the light is given by

$$\boldsymbol{G} = \frac{c}{2L} \frac{1}{(\kappa - i\omega)^2 + \Delta^2} \begin{pmatrix} \kappa - i\omega & -\Delta \\ \Delta & \kappa - i\omega \end{pmatrix}, \qquad (1)$$

*komori.kentaro@jaxa.jp

 ©2021 American Physical Society

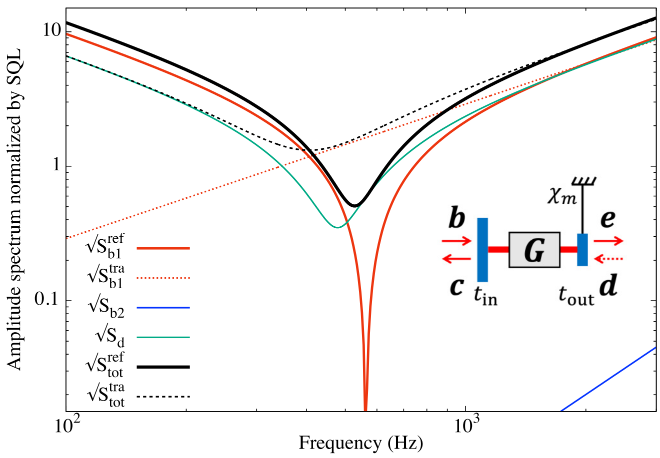

FIG. 1. Amplitude spectra of amplitude and phase fluctuations in reflection and transmission measurement. The definition of the optical fields are described in the inset with the cavity matrix and the mechanical susceptibility. Contributions of the input amplitude fluctuation at the reflection ($S_{b_1}^{\rm ref}$), the input phase fluctuation (S_{b_2}), and the vacuum from the output (S_d) are shown as red (sharp dip), blue (right bottom), and green lines (lower gentle dip), respectively. Total sensitivities at the reflection ($S_{\rm tot}^{\rm ref}$) is represented as a black (top) solid line. The input amplitude ($S_{b_1}^{\rm ref}$) and the total ($S_{\rm tot}^{\rm tra}$) at the transmission are plotted by red (lower) and black (upper) dotted lines.

where L is the cavity length, $\kappa = (t_{\rm in}^2 + t_{\rm out}^2)c/(4L)$ is the total cavity decay rate, Δ is the cavity detuning, and c is the speed of light. In this Letter we define the sign of the cavity detuning with positive restoring force (blue detuning) as plus. Unlike the usual treatment in nano-optomechanics [43], we specialize to the case of macroscopic optomechanical systems where the mirror's motional frequency is so low that its utility as a force transducer necessitates measurement frequencies above its resonance. In this case the mirror motion is in the free-mass regime, i.e., its displacement response to a force is $\chi_{\rm m} \simeq -1/(m\omega^2)$, where m is the effective mass of the mirror.

Here we focus on measurement of the amplitude quadratures at reflection and transmission, in other words c_1 and e_1. The sensitivity on these amplitude measurements of the reflection and transmission normalized by the SQL can be separated by the contributions of $\boldsymbol{b}$ and $\boldsymbol{d}$ as

$$S_{\rm tot}^{\rm ref} = \varepsilon_1 S_{b_1}^{\rm ref} + \varepsilon_2 S_{b_2} + S_d, \tag{2}$$

$$S_{\rm tot}^{\rm tra} = \varepsilon_1 S_{b_1}^{\rm tra} + \varepsilon_2 S_{b_2} + S_d, \tag{3}$$

where ε_1 and ε_2 are relative shot noise levels of the amplitude and phase of the input light. These spectra are given by [44]

$$S_{b_1}^{\rm ref} = \frac{(\kappa^2+\Delta^2)\{\Delta\iota - [(\kappa-2\kappa_{\rm in})^2+\Delta^2]\omega^2\}^2}{16\iota\kappa_{\rm in}(\kappa-\kappa_{\rm in})^2\Delta^2\omega^2}, \tag{4}$$

$$S_{b_1}^{\rm tra} = \frac{\kappa_{\rm in}(\kappa^2+\Delta^2)\omega^2}{\iota\Delta^2}, \tag{5}$$

$$S_{b_2} = \frac{\kappa_{\rm in}\omega^4}{\iota(\kappa^2+\Delta^2)}, \tag{6}$$

$$S_d = \frac{[\Delta\iota - (\kappa^2+\Delta^2-2\kappa\kappa_{\rm out})\omega^2]^2}{4\iota\kappa_{\rm out}\Delta^2\omega^2} + \frac{\kappa_{\rm out}\omega^2}{\iota}, \tag{7}$$

where

$$\iota = \frac{4Pk_0}{mL} \tag{8}$$

shows the optomechanical coupling strength with the intracavity power P and the wave number of light $k_0 = 2\pi/\lambda$. The input and output coupler are given by $\kappa_{\rm in} = t_{\rm in}^2\kappa/(t_{\rm in}^2 + t_{\rm out}^2)$ and $\kappa_{\rm out} = \kappa - \kappa_{\rm in}$ respectively. The amplitude spectra, normalized by the SQL, from the input fluctuation and the vacuum from the output port are plotted in Fig. 1 with the total ones. Here we assume that the input fluctuation is at the vacuum level, $\varepsilon_1 = \varepsilon_2 = 1$. Parameters are as follows: the laser wave length $\lambda = 1064$ nm, $L = 10$ cm, $m = 10$ mg, $\kappa/(2\pi) = 0.25$ MHz, $\kappa_{\rm in}/\kappa = 0.8$, $\Delta = \kappa/\sqrt{3}$, and $P = 1$ W.

The sensitivity at the reflection reaches below unity, which means beating the SQL, due to the dip in $S_{b_1}^{\rm ref}$. This noise reduction occurs at the frequency where the amplitude fluctuation of the direct reflection and that of the cavity leakage are canceled each other. The latter is dominant in the overcoupled cavity at high frequencies, while the former is larger at low frequencies because of the optical spring. The dip frequency is given by

$$\omega_{\rm dip} = \sqrt{\frac{\Delta\iota}{(\kappa-2\kappa_{\rm in})^2+\Delta^2}}, \tag{9}$$

and it is always larger than the resonant frequency of the optical spring. As for the input phase fluctuation shown by the blue line in Fig. 1, the contribution to the total noise is much smaller than the others so that it is negligible. In this Letter, we demonstrate the dip-shaped spectrum of the amplitude fluctuation, which is the most critical to the better force sensitivity at the quantum level.

We discuss difference between the reflection and transmission measurement. As shown by the dotted lines in Fig. 1, the noise from the input amplitude fluctuation at the transmission is smaller than that at the reflection ($S_{b_1}^{\rm tra} < S_{b_1}^{\rm ref}$), resulting in slightly better total sensitivity at low frequencies. This type of back action evasion was experimentally demonstrated by the previous work [40]. Comparing with the transmission measurement, the reflection measurement has an advantage of achieving better force sensitivity ultimately. The sensitivity of the typical overcoupled cavity is better at the dip frequency in the reflection measurement than at low frequencies in the transmission measurement. In addition, beating the SQL is a unique benefit of the reflection measurement.

III. EXPERIMENTAL PROOF OF PRINCIPLE

We demonstrate the proof-of-principle of the technique mentioned above in the experiment depicted in Fig. 2. A 11-cm linear cavity consists of an 8-mg end mirror (0.5 mm thick with a diameter 3 mm) suspended by a single carbon fiber (6 μm thick and 2 cm long), and a much heavier (60 g) input mirror. The test mass consists of the double suspension to isolate it from the seismic motion. The intrinsic Q value of a single pendulum only with the carbon fiber and the mirror is measured to be $Q \sim 8\times10^4$ at the intrinsic mechanical resonant frequency $\omega_{\rm m}/(2\pi) \sim 3$ Hz.

The radii of curvature of the mirrors are 10 cm, shorter than the cavity length of 11 cm; this autonomously stabilizes

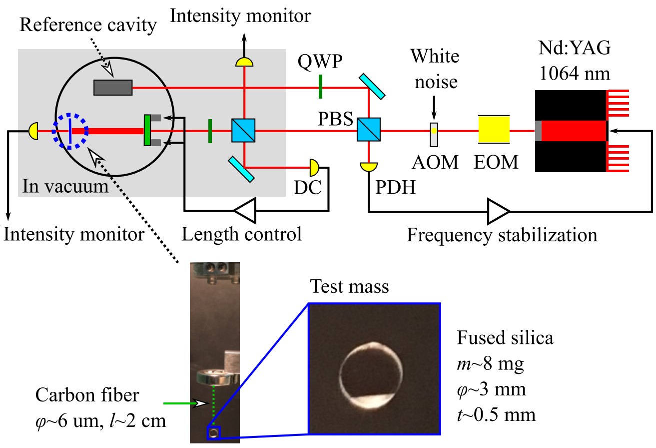

FIG. 2. Schematic overview of the experimental setup. The test mass mirror made of fused silica shown by the photograph is the lowest part of the double suspension. We use the output of a 1064-nm laser. Reflected light from the main cavity is split and detected by a polarizing beam splitter (PBS), a quarter wave plate (QWP), and a DC photodiode. The error signal controls the cavity length with the feedback to the input mirror with the coil-magnet actuator. The classical radiation pressure and intensity noises are excited by the injection of the white noise to an acousto-optic modulator (AOM). The transmission of the cavity is monitored to estimate the cavity detuning during the measurement. An electro-optic modulator (EOM) generates the phase modulation for the frequency stabilization with a reference cavity and a Pound-Drever-Hall (PDH) error signal.

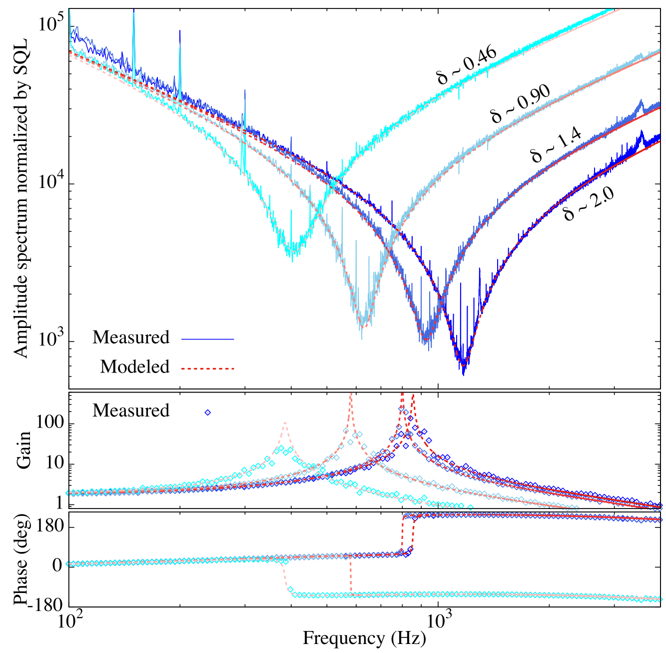

FIG. 3. Demonstration of the dip-shaped spectrum from the amplitude fluctuation of the input light. The amplitude spectrum normalized by the SQL is shown at the upper panel, and the open loop transfer function is shown at the middle and bottom panels. The experiment is performed in four different detunings, and the results (blue solid curves and points) are fitted by the modeled curves (red dotted lines). The estimated normalized detunings ($\delta \equiv \Delta/\kappa$) are written along the measured spectra.

the cavity against radiation-pressure torque instabilities [45]. In order to realize the optical spring, the laser is blue-detuned from cavity resonance. The required error signal to stabilize the detuning is derived from the power reflected from the cavity away from resonance. The error signal is compared against a DC reference, which is then fed back to actuate on coil-magnet actuators on the input mirror that controls the cavity length. By changing the DC reference, we measure several sensitivities to the external force acting on the test mass with different detunings. The transmission of the cavity is monitored to estimate the detuning during the measurement. The cavity is driven by the input power $P_{\text{in}} \simeq 4.7$ mW of 1064-nm light from a Nd:YAG laser derived at a beam splitter. The finesse is measured to be $\mathcal{F} = (3.0 \pm 0.3)\times 10^3$, resulting in the intracavity power $P \sim 5$ W.

The system is not in a regime where quantum radiation pressure fluctuations dominate the motion of the end mirror. Nevertheless, the principle underlying coherent radiation pressure noise cancellation can be demonstrated on calibrated classical radiation pressure noise impressed on the input light. The injection is performed by adding the white noise to an acousto-optic modulator (AOM) the input light passes through, so that the mg-scale test mass is driven by the classical radiation pressure noise. It is confirmed by coherence between the error signal and the intensity noise, which is taken by the photodetector for the light picked off just before the cavity. The injected noise is so large [$\sqrt{\varepsilon_1} \sim O(10^3)$] that the coherence is measured to be almost unity at all frequencies.

In order to observe the classical radiation pressure fluctuation with better signal-to-noise ratio, the laser frequency is stabilized by a reference cavity (4.4 cm long, with a finesse 6.4×10^4). The reflected light from the reference cavity, whose phase is modulated by an electro-optic modulator (EOM), is used as the Pound-Drever-Hall (PDH) error signal. Produced feedback signal actuates a laser piezoelectric transducer and stabilizes the frequency noise. The reference cavity is colocated with the experimental cavity, on a vacuum vibration isolation platform. The pressure is kept around 100 Pa to avoid the coupling of acoustic noise and simultaneously make the cavity locked more easily due to the residual gas damping. This pressure introduces the additional viscous thermal noise, while it is still much smaller than the noise caused by the intensity fluctuation.

IV. RESULT AND DISCUSSION

Our experiments are performed with four different detunings keeping the constant input power. The result of the four measurements is shown in Fig. 3. At the upper panel, the measured spectra normalized by the SQL are plotted with the modeled curves and detunings estimated by the transmission monitor. Those are calibrated from the error signal to the force sensitivity by the transfer function of the open loop and the filter for the length control. The gains and phases of the open loop transfer function are plotted at the middle and bottom panels with the modeled curves. At the resonant frequency, the phase is advanced (delayed) in the two measurements with higher (lower) intracavity power, since the negative damping of the optical spring does (not) overwhelm the residual gas

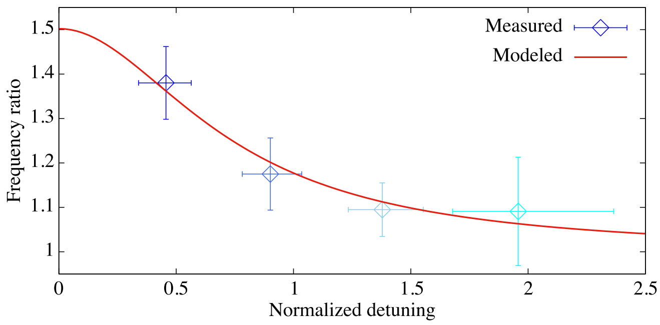

FIG. 4. Ratios between optical spring frequencies and dip frequencies. The four blue dots with errors represent the results with the different detunings. Each colored dot corresponds to the estimation from the same colored spectrum in Fig. 3. The red line shows the modeled curve fitted to the measured data.

damping. The negative damping is compensated by the electrical feedback loop.

In the case of the conventional phase measurement in this setup, we should see the flat force sensitivity without the normalization because of the classical radiation pressure noise. In our experiment, the dip-shaped reduction of the noise is clearly observed by the amplitude measurement of the reflection. Without the detuning fluctuation during the measurement, the sensitivity with injection of the white intensity noise has the spectrum of

$$\sqrt{S_{b_1}^{\mathrm{ref}}(\omega_{\mathrm{dip,m}})} \propto \frac{\left|\omega_{\mathrm{dip,m}}^2-\omega^2\right|}{\omega_{\mathrm{dip,m}}^2}, \tag{10}$$

where $\omega_{\mathrm{dip,m}}$ is the measured dip frequency. In practice, the detuning is changing so that the dip gets thicker. In order to estimate the dip frequency with the error, we assume that the dip frequency distributes as Gaussian where the central frequency is $\omega_{\mathrm{dip,m}}$ with the standard deviation of $\delta\omega$. The modeled curve is generated by averaging the two distributed spectra because of the Gaussianity, $\sqrt{[S_{b_1}^{\mathrm{ref}}(\omega_{\mathrm{dip,m}}+\delta\omega)+S_{b_1}^{\mathrm{ref}}(\omega_{\mathrm{dip,m}}-\delta\omega)]/2}$, and the fitting is performed by the two parameters and the overall factor. In this way, for instance, we estimate the dip frequency in the measurement with the highest power as $\omega_{\mathrm{dip}}/(2\pi) = 1180 \pm 70$ Hz.

In Fig. 4, we show ratios between optical spring frequencies and dip frequencies at the four different detunings. The ratio is a solid indicator to evaluate the system since it is not affected by uncertainty of the intracavity power. The mean values and errors of the ratio are calculated from the modeling of the measured spectra in the previous paragraph. The detunings are estimated by comparing the transmission of the cavity during the measurement with the maximum output in the cavity scan. The errors of the detunings come from the residual fluctuations of the transmission power. When we make the modeled curve of the ratio, the effect of the mode mismatch between the cavity TEM00 mode and the input beam must be taken into account. The mismatched light is directly reflected from the cavity, and contributes as the sensing noise which has a dip at the optical spring frequency [44]. Due to this effect, the measured dip frequency is smaller than that in the perfect mode matching. The mode matching ratio is measured to be $\eta = 92\%$. The transmission of the input mirror is estimated to be $\kappa_{\mathrm{in}}/\kappa = 0.81$ by the fitting.

At the end of this Letter, we discuss future prospect of the experiment. In order to realize the dip-shaped reduction of the intensity noise at the quantum level beyond the SQL, we need a suspended mirror with the higher Q-value pendulum resulting in the lower thermal noise to open the SQL window. The required Q value is roughly 10^6, which has been already achieved by the similar mg-scale pendulum using the monolithic 1-μm silica fiber attached to the silica mirror [46]. Besides, the ng-scale cantilever [47] has observed the quantum radiation pressure fluctuation in broadband frequencies so that the demonstration can be performed immediately at the quantum level. Improving the thermal noise is required to beat the SQL as well by increasing the mechanical Q value or operating the system at cryogenic temperature.

V. CONCLUSION

The optomechanical cavity can be used for the precise measurement of forces acting on mechanical oscillators, such as the quantum decoherence phenomena and the dark matter interaction, while the sensitivity is fundamentally limited by the quantum noise. We theoretically show that the force sensitivity of the test mass trapped by the optical spring can be improved as the dip by measuring the amplitude of the light reflected from the overcoupled detuned cavity. We experimentally demonstrate the dip-shaped improvement with the mg-scale suspended mirror by adding the intensity modulation to the light. This method does not require additional setup for the squeezed light or homodyne measurement. We conclude that the amplitude measurement of the reflection gives a simple way to improve the sensitivity even beyond the quantum limit.

ACKNOWLEDGMENTS

We thank V. Sudhir for help with the manuscript and fruitful discussions. We would like to acknowledge R. Yamada, B. Lane, N. Mavalvala, and K. Somiya for discussions. We also thank OptoSigma company for producing the mg-scale curved mirror. This work was supported by JST CREST Grant No. JPMJCR1873.

[1] H. Cavendish, Philos. Trans. R. Soc. **88**, 469 (1798).
[2] D. J. Kapner, T. S. Cook, E. G. Adelberger, J. H. Gundlach, B. R. Heckel, C. D. Hoyle, and H. E. Swanson, Phys. Rev. Lett. **98**, 021101 (2007).
[3] S. Schlamminger, K.-Y. Choi, T. A. Wagner, J. H. Gundlach, and E. G. Adelberger, Phys. Rev. Lett. **100**, 041101 (2008).
[4] N. Matsumoto, S. B. Cataño-Lopez, M. Sugawara, S. Suzuki, N. Abe, K. Komori, Y. Michimura, Y. Aso, and K. Edamatsu, Phys. Rev. Lett. **122**, 071101 (2019).
[5] T. Westphal, H. Hepach, J. Pfaff, and M. Aspelmeyer, Nature (London) **591**, 225 (2021).
[6] D. Rugar, C. S. Yannoni, and J. A. Sidles, Nature (London) **360**, 563 (1992).

[7] D. Rugar, R. Budakian, H. J. Mamin, and B. W. Chui, Nature (London) **430**, 329 (2004).
[8] B. P. Abbott *et al.* (LIGO Scientific Collaboration and Virgo Collaboration), Phys. Rev. Lett. **116**, 061102 (2016).
[9] B. P. Abbott *et al.* (LIGO Scientific Collaboration and Virgo Collaboration), Phys. Rev. Lett. **119**, 161101 (2017).
[10] Y. Chen, J. Phys. B: At. Mol. Opt. Phys. **46**, 104001 (2013).
[11] M. Aspelmeyer, T. J. Kippenberg, and F. Marquardt, Rev. Mod. Phys. **86**, 1391 (2014).
[12] L. Diósi, Phys. Lett. A **105**, 199 (1984).
[13] R. Penrose, Gen. Relat. Gravit. **28**, 581 (1996).
[14] A. Bassi, A. Großardt, and H. Ulbricht, Class. Quantum Grav. **34**, 193002 (2017).
[15] W. Marshall, C. Simon, R. Penrose, and D. Bouwmeester, Phys. Rev. Lett. **91**, 130401 (2003).
[16] A. Al Balushi, W. Cong, and R. B. Mann, Phys. Rev. A **98**, 043811 (2018).
[17] A. Bassi, K. Lochan, S. Satin, T. P. Singh, and H. Ulbricht, Rev. Mod. Phys. **85**, 471 (2013).
[18] L. Diósi, Phys. Rev. Lett. **114**, 050403 (2015).
[19] S. Nimmrichter, K. Hornberger, and K. Hammerer, Phys. Rev. Lett. **113**, 020405 (2014).
[20] M. Carlesso, A. Bassi, P. Falferi, and A. Vinante, Phys. Rev. D **94**, 124036 (2016).
[21] B. Helou, B. J. J. Slagmolen, D. E. McClelland, and Y. Chen, Phys. Rev. D **95**, 084054 (2017).
[22] K. Komori, Y. Enomoto, C. P. Ooi, Y. Miyazaki, N. Matsumoto, V. Sudhir, Y. Michimura, and M. Ando, Phys. Rev. A **101**, 011802(R) (2020).
[23] D. Carney *et al.*, Quantum Sci. Technol. **6**, 024002 (2021).
[24] F. Monteiro, G. Afek, D. Carney, G. Krnjaic, J. Wang, and D. C. Moore, Phys. Rev. Lett. **125**, 181102 (2020).
[25] Y. Michimura, T. Fujita, S. Morisaki, H. Nakatsuka, and I. Obata, Phys. Rev. D **102**, 102001 (2020).
[26] S. Morisaki, T. Fujita, Y. Michimura, H. Nakatsuka, and I. Obata, Phys. Rev. D **103**, L051702 (2021).
[27] J. Manley, M. D. Chowdhury, D. Grin, S. Singh, and D. J. Wilson, Phys. Rev. Lett. **126**, 061301 (2021).
[28] C. M. Caves, Phys. Rev. D **23**, 1693 (1981).
[29] H. J. Kimble, Y. Levin, A. B. Matsko, K. S. Thorne, and S. P. Vyatchanin, Phys. Rev. D **65**, 022002 (2001).
[30] A. Buonanno and Y. Chen, Phys. Rev. D **64**, 042006 (2001).
[31] A. Buonanno and Y. Chen, Phys. Rev. D **65**, 042001 (2002).
[32] M. J. Yap, J. Cripe, G. L. Mansell, T. G. McRae, R. L. Ward, B. J. J. Slagmolen, P. Heu, D. Follman, G. D. Cole, T. Corbitt, and D. E. McClelland, Nat. Photon. **14**, 19 (2020).
[33] M. Tse *et al.*, Phys. Rev. Lett. **123**, 231107 (2019).
[34] F. Acernese *et al.* (Virgo Collaboration), Phys. Rev. Lett. **123**, 231108 (2019).
[35] V. Sudhir, R. Schilling, S. A. Fedorov, H. Schütz, D. J. Wilson, and T. J. Kippenberg, Phys. Rev. X **7**, 031055 (2017).
[36] N. S. Kampel, R. W. Peterson, R. Fischer, P.-L. Yu, K. Cicak, R. W. Simmonds, K. W. Lehnert, and C. A. Regal, Phys. Rev. X **7**, 021008 (2017).
[37] D. Mason, J. Chen, M. Rossi, Y. Tsaturyan, and A. Schliesser, Nat. Phys. **15**, 745 (2019).
[38] Yu, Haocun *et al.*, Nature (London) **583**, 43 (2020).
[39] F. Y. Khalili, H. Miao, H. Yang, A. H. Safavi-Naeini, O. Painter, and Y. Chen, Phys. Rev. A **86**, 033840 (2012).
[40] J. Cripe, T. Cullen, Y. Chen, P. Heu, D. Follman, G. D. Cole, and T. Corbitt, Phys. Rev. X **10**, 031065 (2020).
[41] C. M. Caves and B. L. Schumaker, Phys. Rev. A **31**, 3068 (1985).
[42] T. Corbitt, Y. Chen, and N. Mavalvala, Phys. Rev. A **72**, 013818 (2005).
[43] T. Botter, D. W. C. Brooks, N. Brahms, S. Schreppler, and D. M. Stamper-Kurn, Phys. Rev. A **85**, 013812 (2012).
[44] See Supplemental Material at http://link.aps.org/supplemental/10.1103/PhysRevA.104.L031501 for the detailed analytical calculations of the power spectra and the calculation of the mode-mismatch effect.
[45] T. Kawasaki *et al.* (unpublished).
[46] S. B. Cataño-Lopez, J. G. Santiago-Condori, K. Edamatsu, and N. Matsumoto, Phys. Rev. Lett. **124**, 221102 (2020).
[47] J. Cripe, N. Aggarwal, R. Lanza, A. Libson, R. Singh, P. Heu, D. Follman, G. D. Cole, N. Mavalvala, and T. Corbitt, Nature (London) **568**, 364 (2019).